Boundary-Layer Meteorol (2007) 122:243–261
DOI 10.1007/s10546-006-9111-3

ORIGINAL PAPER

Instability in Lagrangian stochastic trajectory models, and a method for its cure

Eugene Yee · John D. Wilson

Received: 22 September 2005 / Accepted: 1 July 2006 /
Published online: 21 October 2006

Abstract A number of authors have reported the problem of unrealistic velocities ("rogue trajectories") when computing the paths of particles in a turbulent flow using modern Lagrangian stochastic (LS) models, and have resorted to ad hoc interventions. We suggest that this problem stems from two causes: (1) unstable modes that are intrinsic to the dynamical system constituted by the generalized Langevin equations, and whose actual triggering (expression) is conditional on the fields of the mean velocity and Reynolds stress tensor and is liable to occur in complex, disturbed flows (which, if computational, will also be imperfect and discontinuous); and, (2) the "stiffness" of the generalized Langevin equations, which implies that the simple stochastic generalization of the Euler scheme usually used to integrate these equations is not sufficient to keep round-off errors under control. These two causes are connected, with the first cause (dynamical instability) exacerbating the second (numerical instability); removing the first cause does not necessarily correct the second, and vice versa. To overcome this problem, we introduce a fractional-step integration scheme that splits the velocity increment into contributions that are linear (U_i) and nonlinear (U_iU_j) in the Lagrangian velocity fluctuation vector **U**, the nonlinear contribution being further split into its diagonal and off-diagonal parts. The linear contribution and the diagonal part of the nonlinear contribution to the solution are computed exactly (analytically) over a finite timestep Δt, allowing any dynamical instabilities in the system to be diagnosed and removed, and circumventing the numerical instability that can potentially result in integrating stiff equations using the commonly applied explicit Euler scheme. We contrast results using this and the primitive Euler integration scheme for computed trajectories in a drastically inhomogeneous urban canopy flow.

Eugene Yee (✉)
Defence R&D Canada – Suffield, P.O. Box 4000, Medicine Hat, Alberta, T1A 8K6, Canada
e-mail: eugene.yee@drdc-rddc.gc.ca

J. D. Wilson
Department of Earth & Atmospheric Sciences, University of Alberta, Edmonton, Alberta, Canada

Keywords Dynamical instability · Lagrangian stochastic models · Urban canopy flow

1 Introduction

On the basis of Thomson's (1987) "well-mixed condition" we may derive a Lagrangian stochastic (LS) model for the paths of fluid elements in a turbulent flow, and be assured that those paths are statistically consistent with the (given) joint probability density function (pdf) g_a of the flow's Eulerian velocity field. For relatively simple meteorological flows (e.g., the horizontally uniform surface layer and/or convective boundary layer), such models have proven very satisfactory, and in some respects (e.g., ability to properly handle the near field in the vicinity of sources; or, rational inclusion of the influence of velocity skewness) markedly superior to the common Eulerian formulations. For more complex flows, and in particular urban flows, the superiority of the Lagrangian approach is harder to demonstrate, in part because the well-mixed condition does not provide a *unique* three-dimensional (3-D) model, and in part because one is never able to provide the LS model with a complete and true field of the velocity statistics. Indeed, probably in treating them one will have had recourse to an Eulerian *flow* model to compute the statistics of the wind field, and (wherever so) it would present negligible additional burden to include an Eulerian computation, on the same domain and grid, of tracer dispersion from any number of sources. Nevertheless, the flexibility of the Lagrangian approach (grid free; ability to be run forward or backward in time; etc.) remains a favourable factor for these complex flows.

But there appears to be a further difficulty with the complex 3-D LS models as applied in highly disturbed flows, albeit a problem whose existence is not always recognized. The problem is that in some circumstances, along some trajectories, physically unrealistic velocities arise ("rogue trajectories"). In exploring this problem, which we outline below, we shall refer specifically and exclusively to a particular 3-D LS model (i.e., all three Lagrangian velocity fluctuations included); namely, that provided by Thomson himself for fully inhomogeneous, Gaussian turbulence ("Thomson3D-G"). However, we believe that the principles expounded here for dealing with the problem should apply to other LS models. We deal only with *forward*-time LS models, so that the timestep, dt or (where finite) Δt, is to be regarded as positive.

Chronologically, the first report that an LS model may generate unrealistic (large) velocities was probably that of Luhar and Britter (1989), who in modelling vertical motion in the convective boundary layer with a 1-D well-mixed model (and shortly after the enunciation of Thomson's well-mixed criterion), found it necessary to impose an extraneous numerical constraint (i.e., lower bound) on the magnitude of the Eulerian velocity pdf, $g_a(w) \geq g_{\min}$, in order to prevent the occurrence of unrealistic vertical velocities (A. Luhar 1992, personal communication). It is unclear whether or not this necessity arose from their use of a constant timestep that exceeded the decorrrelation time scale near boundaries, or from a dynamical instability of the pertinent (generalized) Langevin equation, which is given in full by Luhar and Britter.[1] The fact that a lower bound needed to be imposed on g_a in order to obtain a numerically stable

[1] An anonymous reviewer has indicated that the need to impose a numerical constraint in the Luhar and Britter (1989) model to prevent occurrence of unrealistic vertical velocities is most probably caused by the dynamical instability of the Langevin equation used here for modelling dispersion in the convective boundary layer.

integration would suggest that the "drift correction" ϕ/g_a in this model produced an explosive (diverging) behaviour possibly owing to the fact that $g_a \to 0$ much faster than $\phi \to 0$ as the vertical velocity $|W| \to \infty$ (even though ϕ in the model was constructed so that $\phi \to 0$ as $|W| \to \infty$).

Naslund et al. (1994) provided computed fields of mean velocity, turbulence kinetic energy (TKE) k and its dissipation rate ϵ to "drive" an LS simulation (specifically, Thomson3D-G) of the mean concentration field due to continuous point sources upwind and downwind from an idealized, rectangular building. Their k–ϵ (eddy viscosity, $\nu_t \propto k^2/\epsilon$) flow model used the "Boussinesq-like" eddy-viscosity approximation to provide the LS model with the following simplified Reynolds stress tensor ($\mathbf{R} \equiv R_{ij} \equiv \overline{u_i' u_j'}$):

$$\overline{u_i' u_j'} = -\nu_t \left(\frac{\partial \overline{u}_i}{\partial x_j} + \frac{\partial \overline{u}_j}{\partial x_i} \right), \quad i \neq j, \tag{1a}$$

$$\overline{u_1'^2} = \overline{u_2'^2} = \overline{u_3'^2} = \frac{2}{3}k. \tag{1b}$$

It is noted that the model for the Reynolds stress tensor used by Nasland et al. (1994) differs from the conventional Boussinesq eddy-viscosity approximation and, as such, the closure approximation used here does not rigorously satisfy coordinate invariance. Naslund et al. (1994) reported "a rather weak dependence of (computed dispersion) on the off-diagonal stresses" and (of more interest to us here) that the Thomson LS model "**becomes unstable**" unless the stress tensor satisfies realizability. Although Nasland et al. appear to claim that their proposed form for the Reynolds stress tensor satisfies realizability (for their problem), this cannot be true in general without imposition of a limiter on the magnitude of the eddy viscosity within the k–ϵ model, as discussed in Vreman et al. (1994). Furthermore, our experience suggests that although realizability of the Reynolds stress tensor is a necessary condition for stability of the Thomson LS model (in the sense of suppressing the existence of "rogue trajectories"), it is certainly not sufficient.

Yet another indication of the problem of "rogue trajectories" is found in Wilson and Yee (2000), who reported LS simulations (again, with Thomson3D-G) of trajectories in a regular staggered array of bluff aluminum plates in a wind tunnel (the computed 3-D flow field stemmed from an eddy-viscosity closure, and the Reynolds stress matrix would have been realizable). Wilson and Yee noted that "Thomson's criteria for LS models do not limit the 'permissible' spatial variability of flow statistics; in principle, arbitrary profiles are accommodated, provided only that the timestep is appropriately small" (note: except in the case of spectral models, numerically modelled flow fields are spatially discontinuous, although even for the latter case, velocity statistics at the grid nodes can be interpolated to the particle positions to give a continuous velocity field as seen by the LS model). However, they were unable to suppress rogue trajectories by mere reduction of the timestep, and eliminated them by re-setting the velocity randomly whenever and wherever the following two conditions occurred simultaneously: namely, (1) velocity deviated by more than ten standard deviations from the local mean, and (2) the conditional mean acceleration did *not* act in the direction needed to restore the velocity back towards the mean. This latter condition

could be thought of, roughly, as equivalent to an effectively *negative* time scale τ in the Langevin equation (i.e., $\mathrm{d}U = -U\mathrm{d}t/\tau + b\mathrm{d}\xi$), so that the drift term, which in the simplest situations exerts a stabilizing influence on velocity, instead causes instability.

The above examples may suffice to convince the reader that the problem of rogue (computational) trajectories has been encountered by many who have performed this type of work. We have mentioned several strategies that have been invoked. Still another has been to suppress the velocity covariances (i.e., drop the off-diagonal terms of the Reynolds stress tensor of the flow). Practically speaking, this is acceptable, for to date there has been no demonstration that it is crucial to retain the velocity covariance for an accurate prediction of the mean concentration field far away from a source. However it is patently not a cure-all, for instability can occur even in a 1-D LS model (witness the work by Luhar and Britter, 1989). None of these strategies for controlling instability is universally successful, and to the best of our knowledge, this is the first attempt to identify the root cause(s) and offer a strategy to overcome the difficulty, albeit one whose general applicability remains to be proven.

2 Generalized langevin equation for well-mixed LS model

Before we begin, we present a short note on the notation that will be used. Bold upper case symbols will be used to denote matrices, and bold lower case symbols will be used to denote vectors. The only exception to this rule is **U** which will be used to denote the Lagrangian velocity fluctuation vector. We shall also employ the Einstein summation convention in which repeated indices are summed (unless otherwise indicated). Roman indices such as i, j, or k can take values of 1, 2, or 3. For any flow variable ϕ, $\overline{\phi}$ will denote the time average and ϕ' the deviation of ϕ from its time-averaged value. Furthermore, $\mathbf{x} \equiv (x_i) \equiv (x, y, z)$, with $i = 1$, 2, or 3 representing the streamwise x, spanwise y, or vertical z directions, respectively. Finally, the symbol "$\sim$" will be used to denote "distributed as", and $N(\mu, \sigma^2)$ denotes a Normal or Gaussian distribution with mean μ and variance σ^2 (or, standard deviation σ).

Consider first the unique, 1-D well-mixed model appropriate to the vertical motion of a fluid element in a neutrally stratified wall shear layer (surface layer), for which we take the approximation that velocity statistics are Gaussian. The increment in stochastic particle velocity ($W(t) = \mathrm{d}Z(t)/\mathrm{d}t$) at time t over a small time increment $\mathrm{d}t$ is given by the classical Langevin equation

$$\mathrm{d}W(t) = -\frac{W(t)}{T_\mathrm{L}}\mathrm{d}t + b\,\mathrm{d}\xi(t), \tag{2}$$

and the increment in the vertical position $Z(t)$ of the particle at time t is

$$\mathrm{d}Z(t) = W(t)\mathrm{d}t, \tag{3}$$

where $\mathrm{d}\xi(t) \sim N(0, \mathrm{d}t)$ is a random Gaussian variate. Here, $\xi(t)$ represents a Wiener process whose increments $\mathrm{d}\xi(t) = \xi(t + \mathrm{d}t) - \xi(t)$ are normally distributed with $\langle \mathrm{d}\xi(t) \rangle = 0$ and $\langle \mathrm{d}\xi^2(t) \rangle = \mathrm{d}t$ where $\langle \cdot \rangle$ denotes an ensemble average (expected value); and (for suitably restricted T_L, b), $W(t)$ is an Ornstein–Uhlenbeck process. Furthermore, T_L is (loosely) a Lagrangian velocity decorrelation time scale, which is parameterized as

$$T_{\mathrm{L}} = \frac{2\sigma_w^2}{C_0 \epsilon(z)}, \tag{4}$$

where C_0 is a "universal" constant, σ_w^2 is the (Eulerian) vertical velocity variance (which is independent of position), and $\epsilon(z) \propto 1/z$ is the rate of dissipation of turbulence kinetic energy (z is the Eulerian vertical coordinate).

The simplest (and most commonly used) time discrete approximation (note: in this paper, we shall ignore boundary conditions) for this Langevin equation is the stochastic generalization of the Euler approximation for ordinary differential equations:

$$\Delta W(t + \Delta t) = -\frac{W(t)}{T_{\mathrm{L}}}\Delta t + \left(\frac{2\sigma_w^2}{T_{\mathrm{L}}}\right)^{1/2} \Delta\xi, \tag{5}$$

$$\Delta Z(t + \Delta t) = W(t)\Delta t, \tag{6}$$

where $\Delta t \ll T_{\mathrm{L}}$ is a finite timestep and $\Delta\xi$ (increment of a Wiener process) is an independent normally distributed random variable with zero mean and variance Δt. Note that, because $\Delta t, T_{\mathrm{L}} > 0$, the drift term ($\Delta W \propto -W$) operates in favour of dynamical stability, for it tends to return the Lagrangian velocity fluctuation towards zero. Most often, a simple explicit Euler integration is used over the step Δt (i.e., all properties are evaluated at the initial position $\big(W(t), Z(t)\big)$ in phase space corresponding to the beginning of the discretization time interval) and the right-hand side(s) permit one to compute $\big(\Delta W, \Delta Z\big)$, and thus $W(t + \Delta t)$, $Z(t + \Delta t)$ at the next discretization time $(t + \Delta t)$. The order of operations is ambiguous but, practically, irrelevant for sufficiently small Δt. Wilson and Flesch (1993) show how the discretization algorithm can be analyzed rigorously, accounting for the finite timestep and for reflection at boundaries. A computed trajectory will comprise a sequence of finite segments, the segments being shorter (spatially and temporally) closer to boundaries, e.g., the ground (Eulerian coordinate $z = 0$).

We have run through the simple case above in order to contrast it with the far more complex algorithm(s) that have sometimes been applied to compute particle dispersion in highly disturbed urban flows. In contrast to the latter case whose Lagrangian dynamics typically involves multiple (and disparate) time scales, the dynamics embodied in Eq. 2 contains only a single (relevant) time scale T_{L}. In stationary Gaussian turbulence, by definition, the velocity fluctuations are jointly Gaussian, and accordingly the probability density function for the Eulerian velocity fluctuation is

$$g_a\left(\mathbf{u}'|\mathbf{x}\right) = \frac{\left[\det\left(\mathbf{R}^{-1}\right)\right]^{1/2}}{(2\pi)^{3/2}} \exp\left(-\frac{1}{2}u_i' R_{ij}^{-1} u_j'\right), \tag{7}$$

where $\mathbf{u}' \equiv (u', v', w')$ and dependence on position $\mathbf{x}$ arises through the spatial variation of the inverse, $\mathbf{R}^{-1}$, of the Reynolds stress tensor. We note that the existence of a Gaussian pdf for the Eulerian velocity fluctuations requires that the Reynolds stress tensor $\mathbf{R}$ has full rank (viz., the rank r of $\mathbf{R}$ is 3) for otherwise $\mathbf{R}^{-1}$ would not exist. Note that if $r = 3$, $\mathbf{R}$ is positive definite. A necessary and sufficient condition for $\mathbf{R}$ to be positive definite is that the underlying Eulerian velocity fluctuations be a physically realizable process. The latter requires that $R_{ii} > 0$; $R_{ij} \leq \left(R_{ii}R_{jj}\right)^{1/2}$, $i \neq j$; and $\det(R_{ij}) > 0$ (no summation over repeated indices). A mathematically equivalent statement of the realizability condition is that all three eigenvalues of the stress tensor $\mathbf{R}$ be positive.

Thomson's 3-D model for the Lagrangian velocity fluctuation[2] for Gaussian turbulence can be expressed

$$\mathrm{d}U_i = \left(T_i^{(0)} + T_{ij}^{(1)} U_j + T_{ijk}^{(2)} U_j U_k\right) \mathrm{d}t + \left(C_0\epsilon\right)^{1/2} \mathrm{d}\xi_i, \tag{8}$$

where

$$T_i^{(0)} \equiv \frac{1}{2}\frac{\partial R_{i\ell}}{\partial x_\ell}, \tag{9}$$

$$\begin{aligned} T_{ij}^{(1)} &\equiv -\frac{1}{2}\left(C_0\epsilon\right) R_{ij}^{-1} + \frac{1}{2} R_{\ell j}^{-1} \frac{\partial R_{i\ell}}{\partial x_k} \overline{u}_k \\ &= -\frac{1}{2} C_0 \epsilon R_{ij}^{-1} + T_{ijk}^{(2)} \overline{u}_k, \end{aligned} \tag{10}$$

$$T_{ijk}^{(2)} \equiv \frac{1}{2} R_{\ell j}^{-1} \frac{\partial R_{i\ell}}{\partial x_k}. \tag{11}$$

Here, $\overline{u}_i$ is the i-th component of the mean Eulerian velocity of the flow. Finally, the particle coordinates evolve according to

$$\mathrm{d}X_i = \left(\overline{u}_i + U_i\right)\mathrm{d}t. \tag{12}$$

We note that $T_{ij}^{(1)}$ is effectively an "inverse time scale" matrix for relaxation of the velocity fluctuations towards zero. The inverse characteristic time scales (implicit in $T_{ij}^{(1)}$ and controlling relaxation of the velocity fluctuations towards zero, in the context of Eq. 8 or more precisely, in the case that we dropped the quadratic term) are determined by the real parts of the eigenvalues of the matrix $T_{ij}^{(1)}$. For complicated (computed) flow fields, there is no guarantee that the real parts of these eigenvalues are negative,[3] suggesting the existence of unstable (or, exponentially increasing) modes that can lead to an intrinsic instability in the dynamics (so, rather than relaxing towards the state of zero velocity fluctuations, this part of the conditional mean acceleration might cause a rapid (exponential) divergence from this stable state in some direction of **U**). There is nothing in the well-mixed criterion that would preclude the presence of these unstable modes in the dynamics of a well-mixed model, so it is a reasonable possibility that they are one of the causes of the observed rogue trajectories. If we assume these unstable modes are unphysical, then upon eliminating them we should remove the first cause for rogue velocities.

If unstable modes exist in

$$T_{ij}^{(1)} = -\frac{1}{2}\left(C_0\epsilon\right) R_{ij}^{-1} + \frac{1}{2} R_{\ell j}^{-1} \frac{\partial R_{i\ell}}{\partial x_k} \overline{u}_k, \tag{13}$$

then they arise solely from the second term, since provided the Reynolds stress tensor is physically realizable (i.e., positive definite), the first term can only give rise to negative (stabilizing) eigenvalues. As seen in Eq. 9, this second term also appears in $T_{ijk}^{(2)}$, so potentially there are directions in velocity fluctuation space where the quadratic term *also* will contribute unstable (explosive) modes in the dynamics.

[2] The distinction between a model for the increment in Lagrangian *fluctuation* U_i and a model for the increment in *total* velocity $U_i + \overline{u}_i$ can be inferred from $\mathrm{d}\left(U_i + \overline{u}_i\right) \equiv \mathrm{d}U_i + \mathrm{d}\overline{u}_i = \mathrm{d}U_i + \left(\overline{u}_j + U_j\right)\left(\partial \overline{u}_i / \partial x_j\right)\mathrm{d}t$.

[3] The significance of the sign is that only negative eigenvalues have the desirable property of returning the velocity fluctuation towards zero.

In view of all this, we hypothesize that there are two major causes for the observed instabilities; namely, (1) the potential presence of unstable modes that are intrinsic to the dynamical system (likely to be present for the complex flow fields within the urban arrays); and, (2) even in the absence of these unstable modes, the dynamical system for complex flow fields modelled by the stochastic differential equations (SDEs) in this case involves multiple and disparate time scales and, hence, is stiff. Loosely speaking, a 'stiff' system is one whose governing differential equations involve several widely different rate constants or time scales (e.g., τ_1, τ_2 with $\tau_1 \ll \tau_2$). The difficulties that solvers have with stiff differential equations are problems of numerical stability (Garfinkel and Marbach 1977): for the necessity to set the timestep $\Delta t \ll \tau_1$ to render truncation errors tolerable raises the possibility of excessive round-off errors since now Δt is absurdly small relative to the time scale τ_2 of the slowly varying influences. In view of this, the simple explicit Euler scheme used to integrate potentially stiff stochastic differential equations may not keep round-off errors under control, leading (potentially) to a "stochastic" numerical stability problem. Indeed, using an explicit simple Euler scheme to integrate a stochastic differential equation involving disparate time scales will require using an unacceptably small timestep size (smaller than the smallest time scale in the system) in order to maintain the stability of the integration.

In summary, the two mentioned causes for observed instabilities are intimately connected, with the first cause (dynamical instability) exacerbating the second (numerical instability arising from stiffness of the differential equations). Also, even if the first cause was eliminated, the second cause can potentially still exist since multiple and disparate time scales in a system can persist even in the absence of unstable dynamical modes.

3 A fractional-step, semi-analytic time integration scheme

Although methods have been constructed to integrate stiff ordinary differential equations (e.g., Hu 1999; Moore and Petzold 1994), it is difficult to generalize these methods to stiff stochastic differential equations owing to the extreme difficulty of evaluating multiple stochastic (Wiener) integrals with non-constant integrands involving functions of the drift and diffusion coefficients and their derivatives. To integrate the stiff SDEs resulting from application of Thomson3D-G [cf. Eqs. 8 and 12] for the prediction of tracer dispersion in the complex inhomogeneous flows of an urban canopy, we propose the application of a fractional-step semi-analytical time integration scheme. First, given the particle velocity $\mathbf{U}(t)$ at time t, the particle position $\mathbf{X}$ that evolves according to Eq. 12 is updated using an explicit Euler step

$$\mathbf{X}(t+\Delta t) = \mathbf{X}(t) + \Big(\overline{\mathbf{u}}\big(\mathbf{X}(t)\big) + \mathbf{U}(t)\Big)\Delta t. \tag{14}$$

Next, the particle velocity that evolves in accordance with Eq. 8 is updated with the coefficients $T_i^{(0)}$, $T_{ij}^{(1)}$, and $T_{ijk}^{(2)}$ evaluated at the newly-updated position $\mathbf{X}(t+\Delta t)$ [cf. Eq. 14] and these coefficients are then considered to be frozen during the single timestep update of $\mathbf{U}(t)$ to $\mathbf{U}(t+\Delta t)$. The update of the particle velocity is implemented using a fractional-step method in which a timestep is split up into three sub-steps, and different physical effects are accounted for separately in each substep. The dynamics associated with the constant and linear in $\mathbf{U}$ terms as well as the stochastic forcing term are accounted for in the first sub-step; and, the dynamics

corresponding to the diagonal and off-diagonal components in the quadratic in $\mathbf{U}$ term are accounted for in the second and third sub-steps, respectively. In consequence, the method of fractional-steps applied to Eq. 8 to get from timestep t to $t + \Delta t$ would involve the following sequence of three updates associated with the three sub-steps, which symbolically can be expressed as follows:

$$\mathbf{U}^{*} = \mathcal{F}_1\big(\mathbf{U}(t), \Delta t\big), \tag{15a}$$

$$\mathbf{U}^{**} = \mathcal{F}_2\big(\mathbf{U}^{*}, \Delta t\big), \tag{15b}$$

$$\mathbf{U}(t + \Delta t) = \mathcal{F}_3\big(\mathbf{U}^{**}, \Delta t\big). \tag{15c}$$

To apply the method of fractional steps to Thomson3D-G, we begin by "splitting" the Lagrangian velocity fluctuation increment as follows:

$$\mathrm{d}U_i = \mathrm{d}U_i^{(1)} + \mathrm{d}U_i^{(2)} + \mathrm{d}U_i^{(3)}, \tag{16}$$

$$\mathrm{d}U_i^{(1)} = \Big(T_i^{(0)} + T_{ij}^{(1)} U_j\Big)\,\mathrm{d}t + (C_0\epsilon)^{1/2}\,\mathrm{d}\xi_i, \tag{17}$$

$$\mathrm{d}U_i^{(2)} = T_{(i)(i)(i)}^{(2)} U_{(i)} U_{(i)}\,\mathrm{d}t, \tag{18}$$

$$\mathrm{d}U_i^{(3)} = T_{ijk}^{(2)} U_j U_k\,\mathrm{d}t, \quad \{i,j,k\}\backslash\{i=j=k\}, \tag{19}$$

where the brackets (i) indicate that there is no summation over the enclosed index. Now, we proceed to demonstrate that the first two contributions to the fractional-step method can be obtained analytically over a finite timestep Δt (viz., there are analytical forms for the mappings $\mathcal{F}_1$ and $\mathcal{F}_2$).

To proceed, we consider the integration scheme for updating $\mathbf{U}$ from t to $t + \Delta t$ for each part or contribution in the velocity fluctuations as if it were the *only* contribution to $\mathrm{d}\mathbf{U}$. For the first piece, the velocity increment would be the solution of (where we use matrix notation, rather than tensor notation)

$$\mathrm{d}\mathbf{U} = \mathbf{a}_0 \mathrm{d}t + \mathbf{A}_1 \mathbf{U}\,\mathrm{d}t + \mathbf{B}\,\mathrm{d}\mathbf{w}, \tag{20}$$

where $\mathrm{d}\mathbf{w} \equiv (\mathrm{d}\xi_1, \mathrm{d}\xi_2, \mathrm{d}\xi_3)$,

$$\mathbf{a}_0 \equiv \frac{1}{2}\frac{\partial R_{ij}}{\partial x_j}, \tag{21}$$

and

$$\mathbf{A}_1 \equiv -\frac{1}{2}\big(C_0\epsilon\big)R_{ij}^{-1} + \frac{1}{2}R_{\ell j}^{-1}\frac{\partial R_{i\ell}}{\partial x_k}\overline{u}_k, \tag{22}$$

$$\mathbf{B} \equiv \big(C_0\epsilon\big)^{1/2}\delta_{ij}. \tag{23}$$

If it happened that $\mathbf{A}_1$ were diagonal, then we would have three separable (i.e., uncoupled, independent, non-interacting[4]) stochastic differential equations for $\mathrm{d}U_1$, $\mathrm{d}U_2$, $\mathrm{d}U_3$, of generic form

[4] In fact, since the coefficients depend on vector position, and vector position of the particle does change during the timestep, in principle this statement is false; but, it is understood that for the purposes at hand, statistical properties of the flow are held fixed along each trajectory segment, taking the values appropriate to (the gridpoint nearest) the position of the particle at the commencement of the timestep (viz., the drift and diffusion coefficients are "frozen" at their values at the beginning of each timestep).

$$\mathrm{d}U(t) = (a_0 + A_1 U(t))\ \mathrm{d}t + B\,\mathrm{d}\xi(t), \tag{24}$$

where the scalars a_0, A_1, and B are constants (more precisely, frozen coefficients). Assuming the coefficient $A_1 < 0$, this is essentially the classical Langevin equation, the term a_0 entailing an additional (constant) acceleration over the timestep. Let $U(t_0)$ be the initial velocity at the beginning of the timestep (which corresponds to time t_0, so $U(t_0) \equiv U_0$). The velocity at the end of the timestep, $U(t_0 + \Delta t)$, for a finite step Δt is stochastic and can be readily obtained as follows. A *solution in realizations* $U(t)$ of Eq. 24 can be constructed by using the integrating factor $\mathcal{K}(t, t_0) = \exp\big(A_1(t - t_0)\big)$ to write the stochastic differential equation for the transformed quantity, $V(t) \equiv F\big(U(t), t\big) = \mathcal{K}^{-1}(t, t_0)U(t)$, which by virtue of the Ito formula[5] (or, equivalently an integration by parts) has the form

$$\begin{aligned}\mathrm{d}\big(\mathcal{K}^{-1}(t, t_0)U(t)\big) = &\left(\frac{\mathrm{d}\mathcal{K}^{-1}(t, t_0)}{\mathrm{d}t}U(t) + \big(a_0 + A_1 U(t)\big)\mathcal{K}^{-1}(t, t_0)\right)\mathrm{d}t \\ &+ B\mathcal{K}^{-1}(t, t_0)\,\mathrm{d}\xi(t).\end{aligned} \tag{25}$$

Noting that

$$\frac{\mathrm{d}\mathcal{K}^{-1}(t, t_0)}{\mathrm{d}t} = -A_1\mathcal{K}^{-1}(t, t_0), \tag{26}$$

it is now straightforward to integrate Eq. 25 to give

$$U(t) = \mathcal{K}(t, t_0)U_0 + \int_{t_0}^{t} \mathcal{K}(t, \tau)a_0\,\mathrm{d}\tau + \int_{t_0}^{t} \mathcal{K}(t, \tau)B\,\mathrm{d}\xi(\tau). \tag{27}$$

Substituting the explicit form for $\mathcal{K}(t, t_0)$ in Eq. 27 and noting that $(t - t_0) = \Delta t$ results in the following solution

$$U(t) \equiv U(t_0 + \Delta t) = \exp\big(A_1\Delta t\big)U_0 - \frac{a_0}{A_1}\Big(1 - \exp\big(A_1\Delta t\big)\Big) + \gamma(t), \tag{28}$$

where

$$\gamma(t) \equiv B\exp\big(A_1 t\big)\int_{t_0}^{t} \exp\big(-A_1\tau\big)\,\mathrm{d}\xi(\tau). \tag{29}$$

It is easy to demonstrate that $\gamma(t)$ is a Gaussian random variable with zero mean and variance

$$\big\langle\gamma^2(t)\big\rangle = \frac{B^2}{2A_1}\Big(\exp\big(2A_1\Delta t\big) - 1\Big), \tag{30}$$

[5] If $\mathbf{U}(t)$ is an Ito process (i.e., determined as the solution of a generalized Langevin equation), then the stochastic process $f(t) = F\big(\mathbf{U}(t), t\big)$ also has an Ito stochastic differential that satisfies the following Ito formula (using matrix notation, rather than tensor notation):

$$\mathrm{d}f(t) = \frac{\partial F}{\partial t}\big(\mathbf{U}(t), t\big)\,\mathrm{d}t + \nabla_{\mathbf{U}}F(\mathbf{U}(t), t)\cdot\mathrm{d}\mathbf{U}(t) + \frac{1}{2}\mathrm{tr}\left\{\partial^2_{\mathbf{U}}F(\mathbf{U}(t), t)\mathbf{B}\mathbf{B}^T\right\}\mathrm{d}t,$$

where $\mathrm{tr}(\cdot)$ denotes the trace operation and superscript "T" denotes the matrix transpose operation. Here, $\mathbf{B}$ refers to the diffusion matrix [cf. Eq. 20] of the generalized Langevin equation of which $\mathbf{U}(t)$ is the solution. Furthermore, it is assumed that $F(\cdot, \cdot)$ is a continuous mapping with continuous partial derivatives $\partial F/\partial t$, $\nabla_{\mathbf{U}}F$ and $\partial^2_{\mathbf{U}}F$.

using the fact that $\langle d\xi(s)\rangle = 0$ and $\langle d\xi(s)d\xi(s')\rangle = \delta(s-s')\,ds\,ds'$. In consequence, $U(t)$ in Eq. 28 is a Gaussian process with mean

$$\langle U(t)\rangle = \exp(A_1\Delta t)U_0 - \frac{a_0}{A_1}\Big(1-\exp(A_1\Delta t)\Big), \tag{31}$$

and variance

$$\Big\langle\Big(U(t)-\langle U(t)\rangle\Big)^2\Big\rangle = \langle\gamma^2(t)\rangle = \frac{B^2}{2A_1}\Big(\exp(2A_1\Delta t)-1\Big), \tag{32}$$

recalling that $t = t_0 + \Delta t$ and $U(t_0) \equiv U_0$.

3.1 Integration of linear term: first step

Now returning to the general case ($\mathbf{A}_1$ not diagonal), due to its second term $\mathbf{A}_1$ is not a symmetric matrix. Accordingly, its eigenvalues are not guaranteed to be real, and $\mathbf{A}_1$ could have one real eigenvalue and two complex eigenvalues occurring as a complex conjugate pair (implying the presence of a resonant or oscillatory mode in the dynamical system). However, experience with a number of (computed) flows about regular and staggered arrays of cubes and other obstacles suggests such instances do not occur, or if they do must be extremely rare.[6] The following integration scheme *assumes* $\mathbf{A}_1$ has three real eigenvalues whose associated eigenvectors form an independent basis set for the velocity fluctuation space. In this case, $\mathbf{A}_1$ has the eigenvalue-eigenvector decomposition

$$\mathbf{A}_1 = \mathbf{S}\Lambda\mathbf{S}^{-1}, \tag{33}$$

where

$$\Lambda = \begin{pmatrix} \lambda_1 & 0 & 0 \\ 0 & \lambda_2 & 0 \\ 0 & 0 & \lambda_3 \end{pmatrix}, \tag{34}$$

gives the eigenvalues of $\mathbf{A}_1$, and the columns of $\mathbf{S}$ contain the corresponding unit eigenvectors (viz., eigenvectors normalized to have unit length). Expressed in the eigenframe of $\mathbf{A}_1$, the Lagrangian velocity fluctuation vector is

$$\mathbf{U}^{\mathrm{rot}} = \mathbf{S}^{-1}\mathbf{U} \tag{35}$$

(with reverse transformation $\mathbf{U} = \mathbf{S}\mathbf{U}^{\mathrm{rot}}$) and Eq. 20 transforms to

$$d\mathbf{U}^{\mathrm{rot}} = \Lambda\mathbf{U}^{\mathrm{rot}}\,dt + \mathbf{S}^{-1}\mathbf{a}_0\,dt + \mathbf{S}^{-1}\mathbf{B}\,d\mathbf{w}. \tag{36}$$

In this frame the velocity components are uncoupled (i.e., we have three independent Langevin equations), but now the components of the stochastic forcing (or, "noise") term are correlated. Applying the technique *mutatis mutandis* described after Eq. 24 above, Eq. 36 can be integrated exactly over one timestep to give

$$\begin{aligned} U_i^{\mathrm{rot}}(t) &\equiv U_i^{\mathrm{rot}}(t_0+\Delta t) \\ &= U_{i,0}^{\mathrm{rot}}\exp(\lambda_i\Delta t) - \frac{k_i}{\lambda_i}\Big(1-\exp(\lambda_i\Delta t)\Big) + \gamma_i(t). \end{aligned} \tag{37}$$

[6] In the unlikely case that $\mathbf{A}_1$ did have positive eigenvalues and/or complex eigenvalues, one might ignore the second term in $\mathbf{A}_1$, rendering it symmetric, and guaranteeing its eigenvalues are real and negative (provided $\mathbf{R}$ is realizable, i.e., positive definite). However, this is a rather drastic step and would undoubtedly lead to a violation of the well-mixed condition for the LS model.

Here, the stochastic forcing $\gamma_i(t)$ has the form

$$\gamma_i(t) = \left(C_0\epsilon\right)^{1/2} \sum_j S_{ij}^{-1} \exp\left(\lambda_i \Delta t\right) \int_{t_0}^{t} \exp\left(-\lambda_i s\right) \mathrm{d}\xi_j(s). \tag{38}$$

Furthermore,

$$\mathbf{k} \equiv k_i = \mathbf{S}^{-1}\mathbf{a}_0, \tag{39}$$

and $U_i(t_0) \equiv U_{i,0}$ and $U_i^{\mathrm{rot}}(t_0) \equiv U_{i,0}^{\mathrm{rot}}$ are the velocities at the start, t_0, of the timestep, in the laboratory and rotated frames, respectively. It is straightforward to show that the stochastic forcing in Eq. 38 (i.e., $\gamma_i(t)$) involves Gaussian random variables with zero mean (i.e., $\langle \gamma_i(t) \rangle = 0$) and variance-covariance matrix

$$\begin{aligned} \langle \gamma_i(t)\gamma_j(t) \rangle &= \frac{\left(C_0\epsilon\right)}{(\lambda_i + \lambda_j)} \left(\sum_k S_{ik}^{-1} S_{jk}^{-1} \right) \left(\exp\left((\lambda_i + \lambda_j)\Delta t\right) - 1 \right) \\ &= \frac{\left(C_0\epsilon\right)}{(\lambda_i + \lambda_j)} \left(\exp\left((\lambda_i + \lambda_j)\Delta t\right) - 1 \right) \delta_{ij}, \end{aligned} \tag{40}$$

where $\sum_k S_{ik}^{-1} S_{jk}^{-1} = \delta_{ij}$ has been used (δ_{ij} is the Kronecker delta function) owing to the fact that $\mathbf{S}$ is an orthonormal (eigenvector) matrix. In deriving Eq. 40, use was made of the fact that $\left\langle \mathrm{d}\xi_i(s)\mathrm{d}\xi_j(s') \right\rangle = \delta_{ij}\delta(s - s')\mathrm{d}s\,\mathrm{d}s'$.

By these steps one can *exactly* integrate the first (linear part) of the generalized Langevin equation. The dynamical system is intrinsically stable if and only if the eigenvalues of $\mathbf{A}_1$ are strictly negative, implying that there are no dynamically unstable (or explosive) modes in the solution. The analytical solution given above also circumvents the potential numerical instability in a finite difference scheme arising from the stiffness of the equations (viz., here the solution over one timestep is calculated exactly without having to resort to a finite difference scheme such as a simple Euler scheme). Nevertheless, it needs to be emphasized the timestep Δt still must be chosen to be smaller than the characteristic time scales of the problem in order to ensure that the fractional change in the background velocity statistics over a timestep is small, so that the particle does not change its position significantly in phase space in any timestep. Eq. 37 after rotation by $\mathbf{S}$ explicitly defines the first update mapping $\mathcal{F}_1$ in Eq. 15a.

3.2 Integration of diagonal part of nonlinear terms: second step

After the previous step accounting for the linear contributions, and using the resultant intermediate estimate $U_i(t)$ as the initial condition at time point t_0 (we may call it $U_i(t_0) \equiv U_i^{0*} \equiv \mathbf{U}_0^*$), we focus on the second piece of the fractional-step method; namely, that associated with the diagonal part of the nonlinear terms which, by virtue of Eqs. 11 and 18, can be written explicitly as

$$\mathrm{d}U_i(t) = \frac{1}{2} U_{(i)}(t) R_{\ell(i)}^{-1} \frac{\partial R_{(i)\ell}}{\partial x_{(i)}} U_{(i)}(t)\,\mathrm{d}t \equiv g_i U_{(i)}^2(t)\,\mathrm{d}t, \tag{41}$$

where the vector field $\mathbf{g} \equiv g_i$ defined by the previous equation is not to be confused with the Eulerian velocity pdf, g_a. This differential equation is readily integrated exactly to give

$$U_i(t) \equiv U_i(t_0 + \Delta t) = \frac{U_i^{0*}}{1 - g_i U_i^{0*} \Delta t}. \tag{42}$$

Equation 42 now explicitly defines the second update mapping $\mathcal{F}_2$ in Eq. 15b of the fractional-step method (and, allows the update of the solution from $\mathbf{U}^*$ to $\mathbf{U}^{**}$). In this case, $\mathcal{F}_2$ can be determined analytically. Note from Eq. 42 that the particle velocity fluctuations can experience a singularity in finite time if $\mathrm{sgn}(g_i) = \mathrm{sgn}(U_i^{0*})$. However, if $\mathrm{sgn}(g_i) = -\mathrm{sgn}(U_i^{0*})$, Eq. 42 is dynamically stable and corresponds to a contraction of the particle velocity fluctuation vector towards zero (viz., the total particle velocity relaxes towards the background mean velocity). The mentioned singularity can always be avoided if one applies the second fractional step *only* if $\mathrm{sgn}(g_i) = -\mathrm{sgn}(U_i^{0*})$. However, this is a radical process in the sense that it alters the equations being solved and may lead to a violation of the well-mixed condition for the LS model. An alternative to avoiding the finite-time singularity would be to restrict the size of the timestep Δt whenever $\mathrm{sgn}(g_i) = \mathrm{sgn}(U_i^{0*})$. For the latter case, it is seen from Eq. 42 that the finite-time singularity can be avoided if the timestep is chosen such that $\Delta t = f \min\big(1/(g_1 U_1^{0*}), 1/(g_2 U_2^{0*}), 1/(g_3 U_3^{0*})\big)$, where $f \in (0, 1)$. This choice of timestep implies that any component of the solution for the update from $\mathbf{U}^*$ to $\mathbf{U}^{**}$ can at most be amplified by the factor $1/(1 - f)$ whenever $\mathrm{sgn}(g_i) = \mathrm{sgn}(U_i^{0*})$.

3.3 Integration of off-diagonal part of nonlinear terms: third step

Finally, we account for the "off-diagonal part" of the quadratic term in a third fractional step, using the simple forward Euler method because no analytical integration is possible. The Euler scheme is applied using the intermediate result of $\mathbf{U}$ obtained in the second fractional step (we may call it $\mathbf{U}^{**}$) as the initial condition for the Euler step. Unlike the first and second fractional steps, there is no guarantee that this part of the update of velocity fluctuations is stable (dynamically and/or numerically). In consequence, the explicit Euler scheme defines the third update mapping $\mathcal{F}_3$ in Eq. 15c, and this is the only mapping that cannot be analytically determined.

3.4 Choice of timestep

In the ordinary Langevin equation given earlier [cf. Eq. (24)], the effective time scale relative to which we must limit the timestep is $1/(-A_1)$, where $A_1 < 0$ (for dynamical stability). In the more general case at hand, we have *three* natural time scales $(-1/\lambda_i)$ defined by the flow statistics, of which the shortest $(-1/\lambda_{\max})$ provides the strongest limit on Δt ($\lambda_{\max}$ is the largest, i.e., least negative eigenvalue of $\mathbf{A}_1$). However, the specification $T_\mathrm{L} = -1/\lambda_{\max}$ is problematical wherever $\lambda_{\max}$ is nearly zero (e.g., in the case of the water-channel flow in the regular array of obstacles—described later—the largest eigenvalue for any cell in the flow domain is $-1.5825 \times 10^{-5}\,\mathrm{s}^{-1}$, implying $T_\mathrm{L} = 63,187$ s), and in practise there are other time scales that limit the timestep (such as convective time scales or inhomogeneity time scales).

Consequently, in the context of the semi-analytical integration of the Langevin equations, we consider that the effective Lagrangian decorrelation time scale is

$$T_\mathrm{L} = \min\left[-\frac{1}{\lambda_{\max}}, \frac{2\sigma_w^2}{C_0 \epsilon}\right]. \tag{43}$$

(or an appropriate generalization, if σ_w^2 is not the smallest of the velocity variances). Then the timestep is limited to be $\Delta t = \mu T_{\mathrm{L}}$ where $\mu \ll 1$.

Finally, it is noted that the background velocity statistics do not change during the simulation. Due to this, the drift coefficients $T_i^{(0)}$, $T_{ij}^{(1)}$, and $T_{ijk}^{(2)}$ and the diffusion coefficient $(C_0\epsilon)^{1/2}$ in Eq. 8 can be computed at the grid nodes used in the numerical representation of the background velocity field before the LS simulation, and hence the cost of the re-evaluation of these coefficients is completely negligible since they can be accessed through a look-up table. Similarly, for the semi-analytical integration of the generalized Langevin equations, the eigenvector–eigenvalue decomposition of Eq. 33 (which depends only on the background velocity statistics) can be computed before the LS simulation, stored, and accessed efficiently through a look-up table. In view of this, the computational effort needed to integrate the generalized Langevin equations of Thomson3D-G using the semi-analytical scheme proposed here is not substantially greater than the effort necessitated by the far simpler Euler scheme.

4 Simulations using fractional-step semi-analytical scheme

The Mock Urban Setting Test (MUST) experiments (Yee and Biltoft 2004) involved an array of shipping containers laid out to form a regular aligned obstacle array on a salt flat at the U.S. Army Dugway Proving Grounds, in Utah. Here, we examine the performance of the fractional-step semi-analytical integration scheme for Thomson3D-G relative to dispersion measurements carried out in a physical simulation of MUST undertaken in a water channel (Fig. 1). The water channel array consisted of 12×10 obstacles; obstacle dimensions were $(X_b, Y_b, H_b) = (11.8, 59.4, 12.4)$ mm, where x is the direction of the mean stream, and the canyon widths were $(X_c, Y_c) = (62.9, 38.5)$ mm. More details of this water-channel experiment can be found in Yee et al. (2006). A k–ϵ turbulence flow model (Lien and Yee 2004) was used to compute an approximate field of velocity statistics for the MUST array, with measured profiles imposed at the upstream boundary; the computational domain included only one column of obstacles, and was continued cross-stream by the application of a periodic boundary condition in the spanwise direction. The mesh over the computational domain was defined by $202 \times 42 \times 44$ coordinate lines along respectively the streamwise, lateral and vertical directions. For each gridpoint, the eigenvalues λ_i and the corresponding eigenvectors of $\mathbf{A}_1$ were computed, along with all other needed variables (e.g., mean velocities $\overline{u}_i$, velocity variances, TKE dissipation rate ϵ, etc.).

Regarding the LS trajectory modelling, we need to specify a value for the Kolmogorov coefficient C_0. To this purpose, it is noted that Thomson's (1987) well-mixed LS model for Gaussian turbulence implies an eddy diffusivity for vertical dispersion in the diffusion limit as the Lagrangian decorrelation time scale T_{L} tends to zero (Sawford and Guest 1988). In particular, for the 2-D and 3-D versions of Thomson's well-mixed LS model for Gaussian turbulence in a neutrally stratified wall shear layer (with cross-covariances between the velocity fluctuations retained), the implied eddy diffusivity in the diffusion limit has the form

$$K_m = \frac{2\left(\sigma_w^4 + u_*^4\right)}{C_0\epsilon}, \tag{44}$$

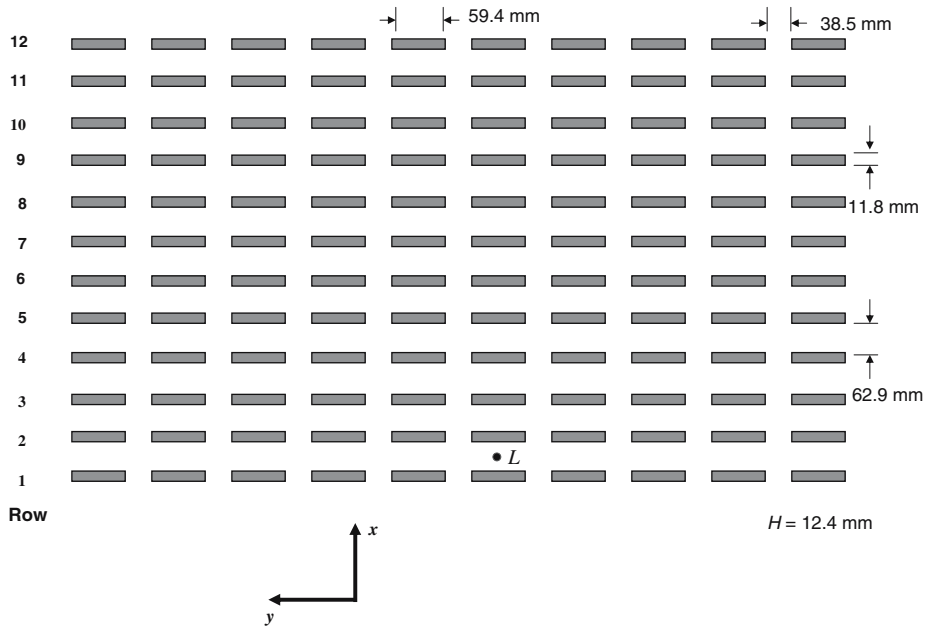

Fig. 1 Configuration of the water-channel MUST experiments (scale of the water channel simulations relative to the atmospheric MUST tests was 1:205). The mean flow was directed along the x-axis, and the tracer point source was at position L for all trajectories of subsequent figures

where u_* is the friction velocity; whereas, for the 1-D version of Thomson's well-mixed LS model for Gaussian turbulence or the 2-D and 3-D versions of this model with the cross-covariances between the velocity fluctuations neglected, the implied eddy diffusivity in the small time scale limit (or, in the far-field limit) has the form

$$K_m = \frac{2\sigma_w^4}{C_0\epsilon}. \tag{45}$$

But for a neutral wall shear layer $K_m = \left(k_v u_* z\right)/S_c$ (where $K \equiv k_v u_* z$ is the eddy viscosity for the neutral surface layer, $k_v \approx 0.4$ is von Karman's constant and S_c is the turbulent Schmidt number) and $\epsilon = u_*^3/k_v z$, so

$$\frac{1}{S_c} = \frac{2}{C_0}\left(\frac{\sigma_w^4}{u_*^4} + 1\right). \tag{46}$$

Interpretation of observations from the experiment Project Prairie Grass indicates that $S_c \approx 0.63$ and using $\sigma_w/u_* \approx 1.3$ in the neutral wall shear layer, we obtain $C_0 = 4.8$ for Thomson3D-G (consistent with the dimensionality of the LS model), which we use for our subsequent simulations (Wilson et al. 2001). It is not necessary to cover other, largely irrelevant details, such as our method for ensuring trajectories are reflected off building "walls". However, we do note that no extraneous interventions were made to control rogue trajectories.

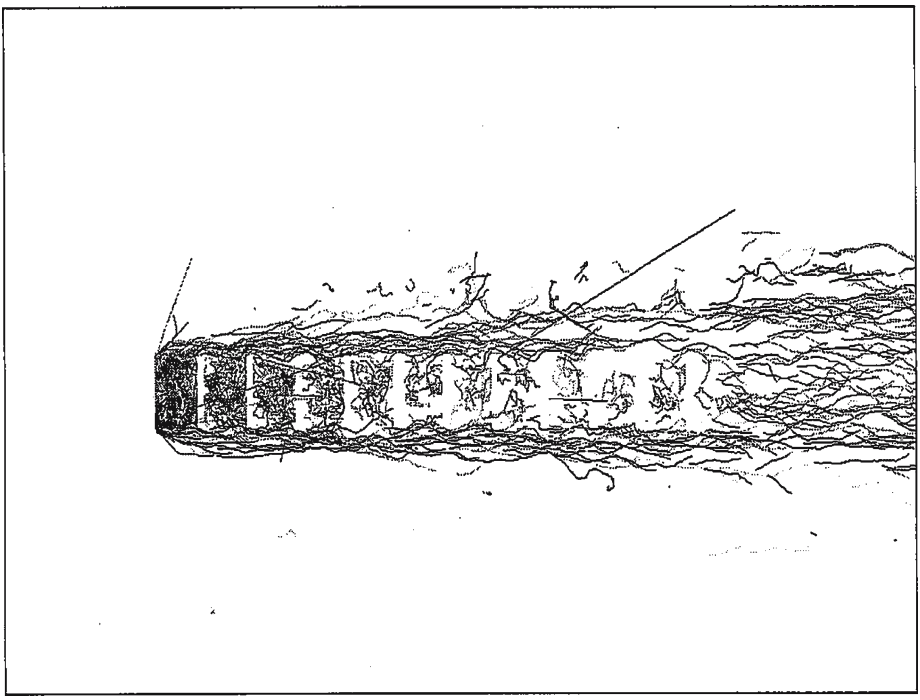

Fig. 2 Trajectories in the MUST array, computed using Thomson's 3-D LS model for Gaussian turbulence. Euler integration with timestep $\Delta t/T_{\mathrm{L}} = 0.1$ was used. No regularization of $\mathbf{R}^{-1}$. Note that a smaller number of paths are shown than on subsequent figures

Figure 2 shows trajectories in the MUST array computed using the simple Euler scheme with a timestep $\Delta t/T_{\mathrm{L}} = 0.1$, and without any regularization[7] of $\mathbf{R}^{-1}$. Particles have been released near ground midway between the two windward-most buildings, and their trajectories are displayed wherever particle height $z/H_b \leq 1$. One can readily identify the straight line paths (indicating excessive velocities, i.e., rogue trajectories), some of which traverse excluded ("building") space—though only due to the fact that the subroutine alluded to does not anticipate that the velocity of inci-

[7] When **R** is nearly singular, its inverse is very sensitive to numerical operations that can introduce numerical noise such as round-off errors. Previously, we had assumed that the observed instabilities in Thomson3D-G were due to a nearly singular **R**, whose inverse is ill-conditioned in the sense that its computation is very sensitive to numerical round-off errors. In consequence, regularization methods must be used to obtain a "stable" inverse of **R** in this case. To this purpose, we applied a truncated singular value decomposition (SVD) of **R** to compute a pseudoinverse of **R** for use in Thomson3D-G in which the contributions of small (near zero) singular values of **R** are discarded in the determination of the "inverse". Needlessly to say, using a truncated SVD to compute a pseudoinverse for **R** did not solve the problem of rogue trajectories.

The singular value decomposition of a matrix **X** of size $m \times n$ is

$$\mathbf{X} = \mathbf{U}\Sigma\mathbf{V}^T, \tag{47}$$

where **U** and **V** are $m \times m$ and $n \times n$ orthogonal matrices, respectively, Σ is an $m \times n$ diagonal matrix with nonnegative singular values $\sigma_j, j = 1, \ldots, \min(m, n)$, arranged in non-increasing order along the diagonal (Golub and Van Loan 1996).

►

Fig. 3 Trajectories in the MUST array, computed using Thomson's 3-D LS model for Gaussian turbulence. A fractional-step semi-analytical time integration with time step $\Delta t/T_{\mathrm{L}} = 0.1$ was used. Upper panel: all terms in generalized Langevin equation retained. Lower panel: off-diagonal part of the nonlinear term of Eq. 19 neglected. The "plume" appears to be wider than that shown in Fig. 2, only because (here) many more paths are shown, including, naturally, a greater number of extreme paths

dence on a building could be so large that, upon reflection, it might proceed through yet another building. This simulation repeatably ended in a program crash.

The upper panel of Fig. 3 shows trajectories in the MUST array, computed using the fractional-step semi-analytical integration scheme (all terms included) and $\Delta t/T_{\mathrm{L}} = 0.1$. Note that, although this simulation does not "freeze" due to program instability, *some* excessive velocities still occurred, carrying particles across excluded building spaces. In contrast, the trajectories of the lower panel, which differ only because the off-diagonal components of the nonlinear terms have been dropped, show no sign whatsoever of instability. Interestingly, trajectories computed with the full semi-analytical integration and with $\Delta t/T_{\mathrm{L}} = 0.01$, are equally acceptable. This would suggest that the observed instability in the off-diagonal components of the nonlinear term arises not from the presence of unstable (explosive) modes inherent in the dynamics, but rather from the presence of multiple and disparate time scales that result in a stiff system of differential equations that need to be integrated numerically in the third step. In this case, use of a sufficiently small timestep (e.g., $\Delta t/T_{\mathrm{L}} = 0.01$) in the explicit Euler scheme would permit a numerically stable integration of the stiff equations.

If it is known *a priori* that no dynamical instability (explosive modes) is present in the dynamics represented by the system of *ordinary* differential equations involving the off-diagonal components of the nonlinear term [cf. Eq. 19], then presumably it would be possible to use a specialized differential solver for the stiff system of equations (e.g., Iserles 1981; Hu 1999; Moore and Penzold 1994), but this would complicate the proposed integration scheme significantly. Furthermore, if it is known *a priori* that no dynamical instability is present in the dynamics represented by constant, linear in $\mathbf{U}$, and stochastic forcing parts of the stochastic differential equation given by Eq. 18, then presumably the analytical solution for this equation over one timestep can be replaced by a stochastic version of a differential solver for a stiff system of ordinary differential equations. However, a stochastic version of a differential stiff solver for Eq. 18 is non-trivial to develop as the solver must necessarily respect the Ito calculus that governs the stochastic forcing term in this equation (Kloeden and Platen 1995).

5 Conclusions

From the preceding discussion we conclude that

- the problem of rogue trajectories subtly hinges on the adequacy of the integration scheme and the dynamics of the generalized Langevin equation;
- the new scheme is guaranteed to eliminate rogue trajectories only if the off-diagonal terms of the nonlinear contribution are eliminated (for the new scheme offers no alternative but the explicit Euler method, for this component), although if the instability in this contribution arises only from the presence of multiple time

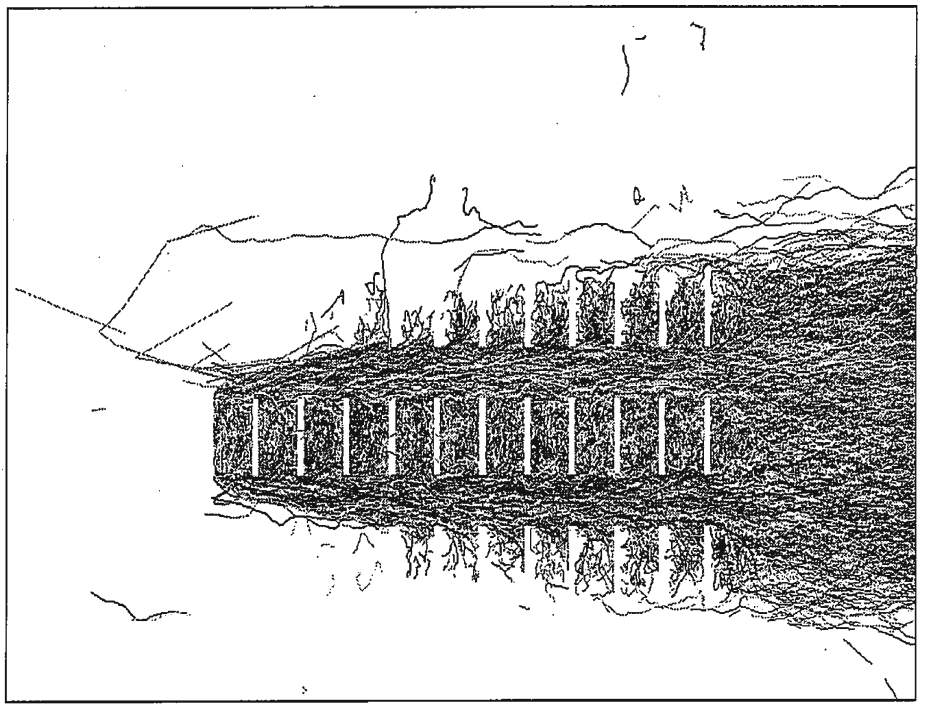

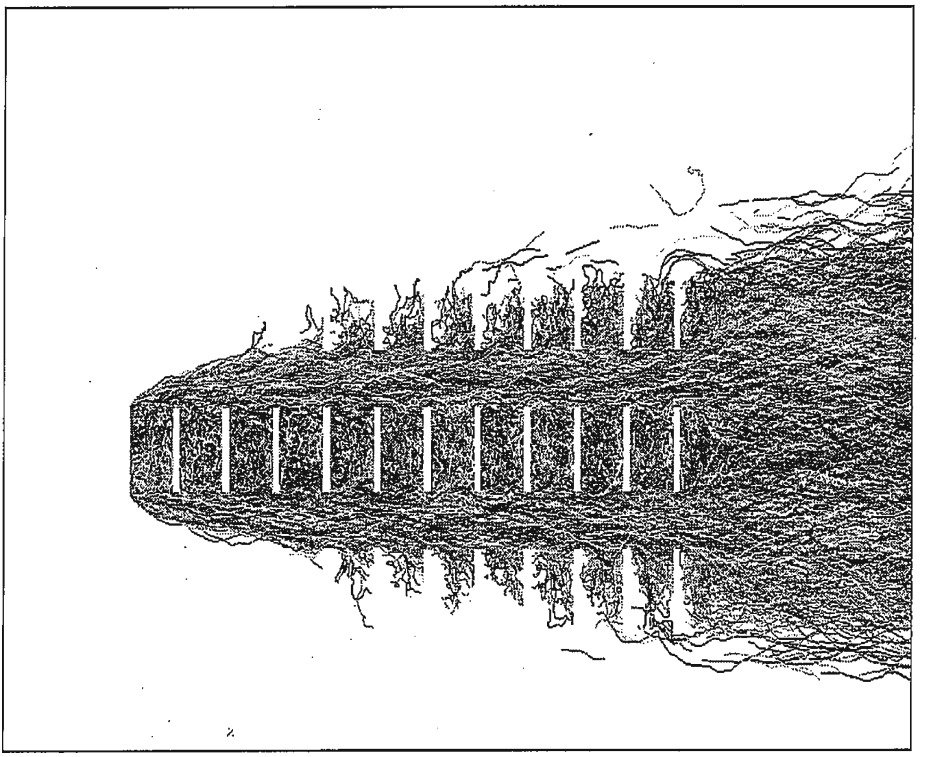

scales in the system rather than from the presence of unstable modes intrinsic to the dynamics, specialized stiff differential equation solvers can be utilized;
– refinement of the timestep will sometimes suffice to suppress unrealistic velocities when using only the explicit Euler scheme for integration of the system of differential equations in the third step;
– the mean concentration field is not necessarily greatly impacted by the occurrence of rogue trajectories.

In closing we note that one of the beauties of the simpler Lagrangian stochastic models is their mathematical and computational simplicity, and that the necessity to invoke the integration scheme laid out here, if necessity it is, penalizes the model in these respects. Unless instability is so severe (in the context of the given flow statistics and the chosen timestep) as to cause floating point errors, some may prefer to live with (a tolerably few) rogue paths, than to program the elaborate steps outlined above, which necessitate (too) the use of ancillary linear algebra software.

Acknowledgements This work was performed under a Chemical Biological Radiological Nuclear Research and Technology Initiative (CRTI) Program under project number CRTI-02-0093RD, and has also been supported in part by research grants from the Natural Sciences and Engineering Research Council of Canada (NSERC) and from the Canadian Foundation for Climate and Atmospheric Sciences (CFCAS).

References

Garfinkel D, Marbach C (1977) Stiff differential equations. Ann Rev Biophy Bioeng 6:525–542
Golub GH, Van Loan CF (1996) Matrix computation, 3rd edn. John Hopkins University Press, Baltimore, MD, 694 pp
Hu C (1999) On the extended one-step schemes for solving stiff systems of ordinary differential equations. Int J Comput Math 70:773–788
Iserles A (1981) Quadrature methods for stiff ordinary differential systems. Math Comput 30:171–182
Kloeden PE, Platen E (1995) Numerical solution of stochastic differential equations. Springer-Verlag, Berlin, 632 pp
Lien F-S, Yee E (2004) Numerical modelling of the turbulent flow developing within and over a 3-D building array, part I: a high-resolution Reynolds-averaged Navier-Stokes approach. Boundary-Layer Meteorol 112:427–466
Luhar AK, Britter RE (1989) A random walk model for dispersion in inhomogeneous turbulence in a convective boundary layer. Atmos Env 23:1911–1924
Moore PK, Petzold LR (1994) Stepsize control strategy for stiff systems of ordinary differential equations. Appl Num Math 15:449–463
Nasland E, Rodean HC, Nasstrom JS (1994) A comparison between two stochastic diffusion models in a complex three-dimensional flow. Boundary-Layer Meteorol 67:369–384
Sawford BL, Guest FM (1988) Uniqueness and universality in lagrangian stochastic models of turbulent dispersion. In: 8th symposium on turbulence and diffusion. American Meteorological Society, Boston, MA, pp 96–99
Thomson DJ (1987) Criteria for the selection of stochastic models of particle trajectories in turbulent flows. J Fluid Mech 180:529–556
Vreman B, Geurts B, Kuerten H (1994) Realizability conditions for the turbulent stress tensor in Large Eddy simulation. J Fluid Mech 278:351–362
Wilson JD, Flesch TK (1993) Flow boundaries in random flight dispersion models: enforcing the well-mixed condition. J Appl Meteorol 32:1695–1707
Wilson JD, Flesch TK, Harper LA (2001) Micro-meteorological methods for estimating surface exchange with a disturbed windflow. Agric For Meteorol 107:207–225
Wilson JD, Yee E (2000) Wind transport in an idealized urban canopy. In: Preprints, 3rd symposium on the urban environment. American Meteorological Society, pp 40–41

Yee E, Biltoft CA (2004) Concentration fluctuation measurements in a plume dispersing through a regular array of obstacles. Boundary-Layer Meteorol 111:363–415

Yee E, Gailis RM, Hill A, Hilderman T, Kiel D (2006) Comparison of wind tunnel and water channel simulations of plume dispersion through a large array of obstacles with a scaled field experiment. Boundary-Layer Meteorol 121, DOI: 10.1007/s10546-006-9084-2, 44 pp